Desalination and Water Treatment
www.deswater.com

1944-3994/1944-3986 © 2012 Desalination Publications. All rights reserved
doi: 10.1080/19443994.2012.698804

Taylor & Francis
Taylor & Francis Group

48 (2012) 130–137
October

Control of membrane biofouling by silver nanoparticles using *Pseudomonas aeruginosa* as a model bacterium

Avital Dror-Ehre[a], Avner Adin[a], Hadas Mamane[b,*]

[a]*Department of Soil and Water Sciences, Faculty of Agriculture, Food and Environment, the Hebrew University of Jerusalem, Rehovot 76100, Israel*
[b]*School of Mechanical Engineering, Tel Aviv University, Tel Aviv 69978, Israel*
Tel. +972 3 6408129; Fax: +972 3 6407334; email: hadasmg@post.tau.ac.il

Received 18 August 2011; Accepted 15 April 2012

ABSTRACT

Biofouling in water systems results in energy loss and potential contamination. In membrane treatments in particular, it often causes flux decline and increases tolerance to cleaning procedures. The effects of exposing bacterial cells to silver nanoparticles on their attachment in the initial stage of biofilm formation and on moderating biofouling buildup in an ultrafiltration membrane apparatus were studied. A high throughput screening method was used for assessing initial bacterial attachment and biofilm formation for *P. aeruginosa* cells exposed to 39 μg/mL of Ag-NPs and compared to non-exposed cells, incubated for 2–48 h. Results showed that Ag-NPs steadily retarded biofilm formation, compared to control cells, where the attached biomass increased over incubation time. To elucidate the influence of Ag-NPs on biofouling buildup in an UF apparatus, two procedures were examined: (a) cells, pre-exposed to Ag-NPs were filtered through a membrane prior to sequential filtration of growth medium, and (b) suspension of cells and growth medium were filtered through a membrane in the presence or absence of Ag-NPs. Exposed samples in both procedures resulted in lower flux decline compared to respective controls. Scanning electron micrographs of post-filtered membranes showed a biofilm layer on the control membrane and scattered individual cells on Ag-NP-exposed membrane.

Keywords: Silver nanoparticles; Biofilm; Biofouling; Ultra-filtration membrane

1. Introduction

Biofouling is the undesired deposition of microorganisms and their secretions (extracellular polymeric substances, EPS) on various surfaces [1]. The phenomenon of biofouling is associated with the existence, properties and activity of biofilm [2]. Biofouling in water systems results in loss of process performance and increased maintenance requirements and cost. In membrane filtration systems, biofouling results in flux decline and requires costly periodic cleaning or membrane replacement [3,4]. Common treatments to prevent or remove biofouling include using oxidative disinfectants or UV irradiation, minimizing nutrients in the feed or altering surface materials to prevent the development of biofilm, or clean-in-place (CIP) to remove mature biofilm. However, limitations such as production of byproducts, increased nutrient availability [5],

*Corresponding author.

poor efficiency against certain microorganisms, development of tolerance, damage to structural materials and more, have given rise to alternative approaches. Biological strategies to control microbial attachment, such as inhibition of the quorum-sensing system or energy uncoupling, enzymatic disruption of extracellular polysaccharides, hydrolysis of cell walls and disruption of biofilm by bacteriophages have created a new research niche in the control of membrane biofouling [6].

Another biofilm control approach is direct pre-interaction of bacterial cells with silver nanoparticles (Ag-NPs) in aqueous suspension, which has been shown to reduce biofilm formation with model bacteria [7]. Nanoparticles (NPs) have unique and distinctive physicochemical properties, including modified structure and a large specific surface, in the range of 1–100 nm [8]. Ag-NPs are reported to exhibit strong antimicrobial activity, including inhibition of microorganism growth in suspension and on solid agar medium [9–11]. On the other hand, Ag-NPs might have a toxic influence on the environment [8,12].

In the water sector – membrane-separation technology in particular – low-fouling coated membranes constitute a growing research area and silver-coated membranes have been characterized as being able to prevent biofouling [4]. Incorporation of Ag-NPs into nanofiltration (NF) and ultrafiltration (UF) membranes made of polysulfone, polyamide and cellulose acetate, among other materials, as well as reverse osmosis (RO) membranes, has been shown to have anti-biofouling ability [4,5,13–15]. The nanocomposite membranes have been characterized mainly as slow biocide-releasing, and their main limitation is loss of silver which requires replenishment [4,15]. Recently, the impact of Ag-NPs on mature biofilm was studied. A reduced biofilm volume with no change in viability of bacterial cells was reported upon exposure of a 3-day-old biofilm to Ag-NPs [16]. The initial phase of biofilm formation – the attachment of microbes to a surface – takes only a few hours [17]. This process is dictated mainly by the bacterial species and its phenotypic and genotypic properties, surface composition and properties, and environmental factors [17]. For example, adhesive strains of *Pseudomonas aeruginosa* have been reported to be hydrophobic while non-adhesive strains are hydrophilic. Moreover, adhesive strains reduce surface tension due to release of surface-active extracellular substances. Conversely, zeta potential and motility are not distinctive related to adhesion [18]. Bacteria-secreted EPS have been mentioned as facilitators in the attachment to solid surfaces such as membranes [6].

This study examined the effect of exposing bacterial cells to Ag-NPs, on their attachment in the initial stage of biofilm formation and on moderating biofouling buildup in an UF membrane apparatus. *P. aeruginosa* cells exposed to Ag-NPs were either (a) seeded on an UF membrane prior to sequential filtration of growth medium; investigating the biofouling buildup in a static bacterial layer and (b) suspension of cells and growth medium were filtered through a membrane in the presence or absence of Ag-NPs; investigating the biofouling buildup in a dynamic bacterial layer – a deposition that accumulates slowly on the membrane.

2. Materials and methods

2.1. Preparation and characterization of Ag-NPs

The synthesis of Ag-NPs is based on reducing metal ions in solution in the presence of a stabilizing agent, trisodium citrate in this study. The preparation methods, characterization of particle size distribution, average particle size and morphology of the particles have been reported previously [7]. The colloidal stability of the particles was verified by UV–Vis spectrometer (Varian Cary 100 Bio), Zetasizer (Malvern Instruments Nano-zs) and by Tecnai F20 TEM (FEI, Eindhoven, The Netherlands).

2.2. Model bacteria and experiment suspensions

A derivative of *P. aeruginosa* PAO1 containing a gene encoding carbenicillin resistance (200 μg/mL) and *P. aeruginosa* ATCC 27853 were used as model bacteria due to their ubiquitousness in water and their frequent presence in biofilms. Carbenicillin is active against a wide spectrum of Gram-negative and Gram-positive bacteria [19] and was used in this study to reduce contamination in the experimental system. Pure cultures of *P. aeruginosa* were grown overnight to an optical density (OD_{600}) of ~0.1 in M9 medium consisting of (in 1 L): 200 mL M9 salts (64 g Na_2HPO_4 $7H_2O$, 15 g KH_2PO_4, 2.5 g NaCl, 5 g NH_4Cl in 1 L), 2 mL 1 M $MgSO_4$, 20 mL 20% (v/v) glucose, 100 μL 1 M $CaCl_2$. M9 was used due to the low fouling contribution of its components. The experimental samples contained bacterial cells suspended in deionized (DI) water and Ag-NPs. A similar suspension without Ag-NPs was used as a control. The suspensions were thoroughly vortexed to allow good interaction between bacterial cells and particles. Each sample was serially diluted in DI water, plated on a LB agar plate and enumerated to determine the number of colony-forming units (CFU) before and after interaction with Ag-NPs.

2.3. Characteristics of bacterial cells – hydrophobicity assessment

To assess the change in hydrophobicity of bacterial cells due to exposure to Ag-NPs, the procedure

described by Rosenberg et al. [20] was generally followed. Pure culture *P. aeruginosa* cells were grown overnight in M9 and then exposed to Ag-NPs. Free Ag-NPs were separated by centrifugation at ~800*g* for 15 min, a condition in which the free Ag-NPs remain suspended and the pellet includes NPs attached to bacterial cells. The pellets (exposed and control) were resuspended in 0.9% (w/v) NaCl and then 3 mL suspension and 600 μL of hexadecane (Fluka Analytical 52210) were vortexed for 30 s in a glass tube. The mixtures were left for 15 min, allowing the hexadecane phase to rise completely. Adherence to hexadecane (%) was measured at 600 nm.

2.4. Biofilm formation and quantification

The effect of Ag-NPs on the initial attachment and formation of biofilm was evaluated using a standard screening assay [21], which allows quantification of attached biomass concurrently in various experimental conditions, as detailed in Dror-Ehre et al. [7]. Attached biomass was presented relative to wells containing DI water, which was considered as zero cell attachment. The experimental samples contained ~10^6 × CFU/mL of *P. aeruginosa* cells suspended in growth medium (M9) in the presence or absence of Ag-NPs (treated and control). To attain a significant decrease in formation of biofilm, the treated cells were exposed, based on previous results [7], to 39 μg/mL Ag-NPs and compared to non-exposed cells (control cells). Various incubation periods were used, in the range of 2–48 h, with a focus on the first 8 h.

2.5. Membrane filtration unit

Formation of biofouling by bacterial cells exposed, or not, to Ag-NPs, was assessed in a membrane filtration apparatus by tracing the change in permeate normal flux (J/J_0) versus time, where J is the permeate flux at time t and J_0 is the permeate flux of ultrapure water for a clean membrane or permeate flux at time zero. Amicon bench-scale dead-end UF cells model 8400 and 8050 (Millipore Corp., USA) operating at constant pressure, were used. The volumes of the cells were 400 and 50 mL and the effective membrane areas were 41.8 and 13.4 cm^2, respectively. Nitrogen (99.999%) was used to force solutions from a 5-L holding tank into the membrane pressure cell. The accumulated permeate water weight with time was recorded by Balint software program and the flux was calculated. A pressure regulator (Precision, SMC, Japan) was used to keep the pressure constant throughout the experimental procedure. The DI water was obtained from an RO water-purification system equipped with photocatalytic UV lamp (Milli-Q Direct system, Millipore); the resistivity of the water was 18 M cm at 25 °C.

2.6. Scanning electron microscopy (SEM)

For SEM imaging, membranes were gently removed from the UF cell at the end of experiments, cut to pieces of ~1 cm^2 and prepared for observation. The membrane pieces were fixed in 2.5% (v/v) glutaraldehyde, then rinsed three times in phosphate buffer saline (PBS) and three times in DI water, and air-dried. The specimens were glued to the SEM stub with carbon adhesive and sputter-coated with gold. Imaging was performed with a Quanta 200 FEG ESEM and analyzed with Oxford-INCA.

3. Results and discussion

3.1. Characterization of Ag-NPs

The Ag-NPs formed stable dispersions and had a roughly spherical shape with a relatively narrow size distribution, verified by TEM micrographs. Two batches of particles were used in the various experiments: type A (mean diameter of 8 ± 2.6 nm) and type B (mean diameter of 9.8 ± 2.9 nm). Fig. 1 shows UV–Vis absorbance spectra (relative to DI water) of the Ag-NPs (type B, 25 μg/mL) before filtration ("feed" relates to a suspension of Ag-NPs, growth medium with bacterial cells and "blank" relates to a suspension of Ag-NPs and growth medium without bacterial cells), and after ("permeate") filtration through a 0.01-μm polycarbonate (PC) membrane. All three groups presented a single broad peak in the typical Ag-NP range (390–420 nm [10]) indicating stable and uniform Ag-NPs, with permeate absorbance, as expected, lower than the feed. Permeate curve

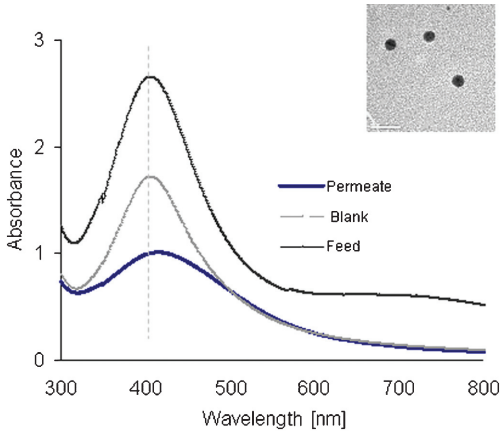

Fig. 1. UV–vis absorbance spectra of Ag-NPs in feed and permeate of UF thought 0.01 μm PC membrane. The inset is a representative transmission electron microscopy (TEM) micrograph showing the shape and size of a few particles (bar = 20 nm).

shows a slight red-shift movement, indicating change in the mean particle size. The change in the mean size is a result of both selective rejection of larger Ag-NPs and of nano-particles' attached to the bacterial cells. ICP-MS (inductively coupled plasma mass spectrometry) analysis of the concentration of Ag in the feed and permeate samples revealed over 85% rejection of the Ag-NPs from the membrane.

The specimen was diluted 10-fold with DI water while preparing the grid for TEM observation, to avoid particle overlap during grid drying. The zeta potential value of the Ag-NPs was –38.8 mV, indicating stable colloids, and the size–distribution histogram was in the range of 2–18 nm. Our previous study showed less biofilm formation when bacterial cells were exposed to similar particles [7].

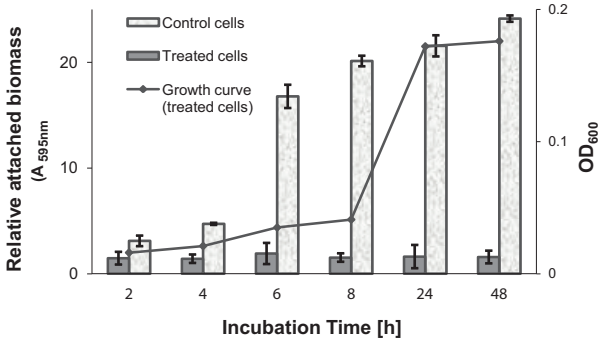

Fig. 2. Attached biomass (relative to assay threshold) verses incubation time.

3.2. Effect of Ag-NPs on initial attachment

A high throughput screening method (detailed in Section 2) was used for elucidating the effect of Ag-NPs on the initial attachment and formation of biofilm. Fig. 2 illustrates the effect of exposure to Ag-NPs on the amount of attached biomass produced by the cells. Attached biomass formed by exposed (treated) and non-exposed (control) cells, was evaluated in relative to DI water (zero attachment). The attached biomass originating from the treated bacterial cells was steady and similar to the assay threshold (DI water), whereas the attached biomass of the control cells increased over time. The growth curve of the surrounding non-attached treated cells, under the same conditions used to grow the attached cells, is also presented in Fig. 2. The non-attached control cells reached the stationary phase in about 24 h. The inferior and limited treated attached biomass was steady in all incubation periods although cells were grown in the surrounding bulk suspension. It should be noted that the quantification assay is unable to (a) distinguish between growth of biofilm cells and new attachment of cells from the surrounding suspension and (b) determine whether the attached cells were dead or alive. However, since the attachment phase is known to be relatively rapid [17], it is reasonable to interpret the increase in the control attached biomass as dominated by biofilm growth rather than by adherence of new cells from the surrounding bulk suspension. Moreover, similar adhesion rates have been reported for dead and live cells [1]. Since the surface and experimental condition were similar for both treated and control tests; the difference in cells attachment may be related to interruption to microbial cell functioning, caused by the presence of Ag-NPs. Specifically, this may result in either interruption to the first weak and transient attachment of cells to surface or interruption to the second stage of attachment, in which irreversible anchoring that produces firm cell–surface attachment take place [17]. This biofilm assay is designed to leave only adherent bacteria in the wells, while removing cells that are not well-anchored. The mechanism that possibly disturbed the attachment (either reversible or irreversible) of the treated cells and the biofilm growth that followed it is not clear. Previous studies demonstrated a stress state of Ag-NPs exposed cells [7]; thus limited anchoring due to inactivation of "biofilm genes" resulting from the stress imposed by the Ag-NPs is a suggested but not yet confirmed mechanism.

Bacterial cell properties are known to influence their attachment to surfaces [17,18] and hydrophobicity is one of the non-specific properties of bacterial cell that plays a major role in the attachment, with the more hydrophobic bacteria having a greater affinity for hydrophobic surfaces (e.g. microtiter plates) [22]). The impact of Ag-NPs on the hydrophobicity of the bacterial cell characteristics was examined as a potential mechanism to explain the effect on initial attachment and biofilm formation. Hydrophobicity of the cells was determined based on their adherence to hexadecane (detailed in Section 1). Results showed that control and treated cells (0 and 50 μg/mL type B Ag-NPs) separated from the non-interacted Ag-NPs, presented 20 ± 3% and 23 ± 1% adherence, respectively. The hydrophobic affinities of the cells did not change due to interaction with Ag-NPs and it seems that hydrophobicity of the bacterial cells does not play an important role in the mechanism of action of Ag-NPs, and other cell expressions are involved.

3.3. Effect of Ag-NPs on creation of biofouling

The influence of exposure to Ag-NPs on development of biofouling was assessed by tracing the change in the normal permeate flux (J/J_0) with time in a UF

membrane cell (model 8400) operating at constant pressure and ambient temperature. Millipore cellulose acetate 1-kDa UF membranes were used due to their low flux, allowing a long filtering period in a closed, undisturbed system. At the beginning of each test, the filtering system was well cleaned by filtering dilute sodium hypochlorite (3%) and ethanol (70%), and then DI water was filtered through the new clean membrane (duplicate) to determine J_0. Ag-NP-exposed (treated sample) and non-exposed (control) *P. aeruginosa* cells were seeded on the membranes by filtration of 15 mL of overnight incubated bacterial suspension; then 5 L of 1:25-diluted M9 medium was sequentially filtered, under constant pressure of 2 ± 0.03 bar, for 60 h. The treated sample was duplicated with two different particle concentrations (15 and 30 μg/mL Ag-NPs type A). The control sample contained ~3.2×10^8 CFU/mL and the treated sample contained ~5.4×10^8. The clean water flux was 7.8 and 8.4 LMH for control and treated samples, respectively. Fig. 3 presents the change in permeate flux (J/J_0) with time. Up to 24 h of filtration, both treated and control samples showed similar permeate fluxes. However thereafter, the flux of the control sample decreased to a greater extent than that of the treated samples. After 48 h of filtration, the 15 μg/mL treated sample also showed flux decline, which might be a result of biofilm that formed on the membrane surface initiated by the seeded bacterial cells, or a result of system contamination. In either case, exposure to Ag-NPs moderated the flux decline.

In the next step another protocol was used to allow continuous interaction between the Ag-NPs and bacterial cells and minimize contamination of the system. The experimental suspensions included the antibiotic Carbenicillin, *P. aeruginosa* PAO1 bacterial cells, M9 and Ag-NPs (treated sample only) that were mixed into the holding tank and then continuously fed into the UF cell. *P. aeruginosa* PAO1 cells were used due to their resistance to Carbenicillin. The layer deposited on the membrane using this technique accumulated dynamically with online active interaction between particles and bacterial cells, in contrast to the static seeded bacterial layer and pre-interaction, in the previous protocol. Experiments were performed in a ~3 times larger surface area UF unit (model 8050) and smaller pore size ratings membranes (Sterlitech 0.01-μm PC UF membrane) to minimize peripheral surface artifacts and to maintain low flow rates, respectively. Poly carbonate (PC) membranes were used since their pore sizes are specific and uniform and they showed less background interruption in microscopic observation. The pressure was kept constant at 0.78 ± 0.01 bar and J_0 as initial flux at time zero was 6.6 and 6 LMH for control and treated samples, respectively. The system was cleaned as in the previous test. The control experimental suspension contained 10 mL overnight bacterial cells at an OD_{600} of 0.117 (4.8×10^7 CFU), 100 mL M9 (1:10 dilution), 1 mL Carbenicillin and DI water filled to 5 L. The treated suspension contained an additional 450 mL of Ag-NPs type B (9 μg/mL), with mean size of about the same size as the membrane pore. The number of Ag-NPs in the 5 L holding tank was estimated at 5×10^{12} (10^9 particles/mL) using Ag density and particles' mean size and concentration. Rejection of Ag-NPs from the membrane was 85% according to ICP analysis of permeate and feed water, leaving approximately 1.5×10^8 particles/mL in the permeate flow. Note that NP rejection reflects membrane rejection as well as secondary rejection by attachment of NPs to bacterial cells.

Once the filtration process started, the foulants held in the holding tank slowly began to arrive at the membrane surface. Some small particles were able to pass through the membrane pore while other constricted the flow through the membrane by complete, intermediate or internal blockage of the pores. These particles could later on accumulate on preceded deposition and forming filter cake, as well. Particles larger than the membrane pore were either accumulated on the membrane surface forming a filter cake or blocking the pore entrance. The potential foulants in the control and treated sample are different. Ignoring the growth medium components and the antibiotic that showed negligible flux decline and are equal in both samples, the control sample held bacterial cells that are larger than the membrane pore while the treated sample held the same bacterial cells (yet, interacted with Ag-NPs) and free Ag-NPs that are two orders smaller than the cells and are about the same size as the membrane pore.

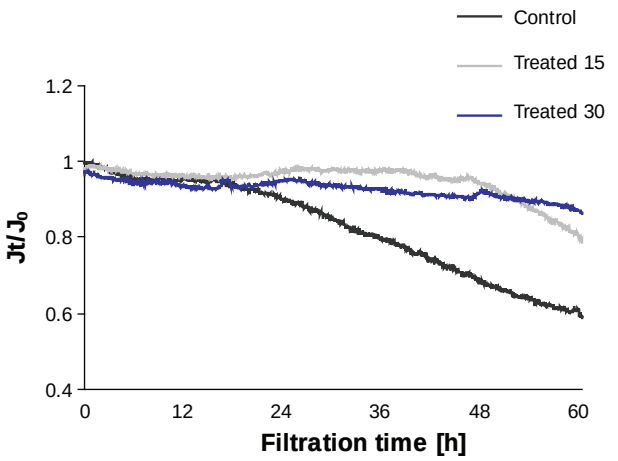

Fig. 3. Normalized permeate flux (J/J_0) verses time for non-exposed or pre-exposed cells to Ag-NPs prior to sequential filtration.

In both samples a time-dependent accumulated resistance to the water flow was built. Fig. 4 presents the normal resistance first derivative with time. The resistance at time zero and time t were derived from the respective flux data using Darcy's law. This law describes the fluid flow through a permeable media as a direct function of surface area and pressure and reverse function of fluid viscosity and resistance. In a constant pressure, area and viscosity, the resistance can be calculated as an inverse ratio of the flux. The first derivative dR/dt obtained by polynomials (order 4–5) smooth of numerical differentiation of the resistance. Fig. 4 shows similar resistance between control and treated samples in the first 6 h of filtration. This period is the time required to form the control biofilm (see Fig. 2). After about 6 hof filtration the change in the resistance built by the control sample started to increase to a greater extent compared to that of the more moderated change in the resistance of the treated sample.

The resistance derived from membrane blocking was previously mentioned to be influenced by three major factors: the amount of particles simultaneously arriving at the membrane surface, the amount of particle accumulation, and the filtration rate [23]. Complementary subfactors as arrival timing, availability of bare membrane surface, crowding produced by previous deposition or neighboring particles, accessibility and opportunity to migrate to the membrane pore, particle motion and others, are also associated with the membrane blocking and thus the three factors are not completely independent. As foulants accumulate, the resistance is constantly changing reducing the flux. Four classic modeling laws, originally developed by Hermia [24] for dead-end filtration process, are widely used to explain the flux behavior under constant pressure filtration. The laws describe four fouling mechanisms: cake filtration and intermediate or standard or complete blocking. Table 1 summarizes the potential foulant components and blocking mechanisms of the two tested suspensions.

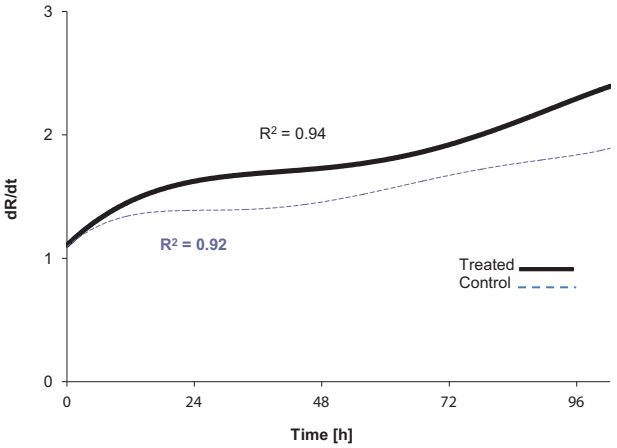

Fig. 4. First derivative of normalized resistance verses time for a suspension of cells and growth medium filtered through a membrane in the presence or absence of Ag-NPs.

In addition to the foulants present in Table 1, EPS produced by cells and bacterial cells co-deposited on the membrane tend to form a biofilm layer with the EPS filling the voids between the cells. This interaction may reduce the portion of membrane area that is available for "bare" filtration and accelerate the formation of a cake layer. Our previous study showed that Ag-NPs interacted bacterial cells formed less biofilm compared to non-interacted cells [7]. And indeed, although the treated sample presents, according to Table 1, a higher fouling potential, results show moderated hydraulic resistance that could be attributed to moderate biofilm formation. All four filtration laws can be written in one form, providing a convenient and commonly used single equation to determine fitting of experimental data to one of the four blocking mechanisms. The form is a time (t)-dependent behavior of cumulative filtrate volume (v) as follows:

$$\left(\frac{d^2t}{dv^2}\right) = k\left(\frac{dt}{dv}\right)^n \tag{1}$$

The parameters n and k are empirical parameters that characterize the fouling mechanism and allow comparing the effect of various factors such as membrane characteristics and nature of foulants. The blocking law exponent, n, defines the fouling mechanisms and the blocking coefficient, k, is associated with the mechanism. For example, surface area and foulants' concentration, diameter and density define the complete blocking coefficient [25]. In this study, two greatly different particle sizes with dissimilar effect on the permeability of the membrane were simultaneously filtered, and more than

Table 1
Estimate summary of potential foulant components and filtration mechanisms

	Control[a]	Treated[a]
Arriving particles	10^5 bacterial cells	10^5 bacterial cells, 10^9 Ag-NPs
Accumulation particles	10^5 bacterial cells	10^5 bacterial cells, 7.6×10^8 Ag-NPs[b]
Potential mechanisms	Complete blocking, Cake filtration	Pore constriction (complete, intermediate and standard), cake filtration

[a]At each 1 mL suspension.
[b]Based on 85% rejection of particles and assuming attachment of 100 particles per each bacterial cell.

one major filtration blocking mechanism is relevant. In such a case an exact matching to Hermia's four models is not expected, yet, the data was analyzed using this model (Eq. (1)) to compare the two samples and to demonstrate a different fouling state. Fig. 5 illustrates the second derivative (d^2t/dV^2) versus the first derivative (dt/dV) for both treated and control membranes. Several values of the second derivative were negative due to the low flow. Since the coefficient k describes physical characteristics such as foulant diameter, negative values are an artifact thus were deleted.

The control sample presents a horizontal line indicating constant second derivative, i.e. $n = 0$, that corresponds in that model to cake filtration results of the developed biofilm layer. A previous study that used this model to interpret biofouling mechanisms showed consisting results, indicated of intermediate blocking in the very early initial stage followed by cake filtration mechanism toward the later stages of filtration [26].

On the other hand, a scatted pattern is observed for the treated sample that does not fit the behavior of any of the individual four blocking filtration laws. Additional more complicated models were developed to consider the effect of deposition of different particles size and the combined effect of two fouling mechanisms [23,27,28]. These models could be further developed to fit and explain the behavior of Ag-NPs interacted with bacterial cells. Blankert et al. [29] presented another approach to analyze combined fouling mechanisms, using the blocking laws as a resistance model instead of flow model, describing the total resistance as a function of the fouling state. This approach may also assist to elucidate the fouling mechanisms of bacterial cells interacted with Ag-NPs.

To further support the assumption of moderated biofilm formation in the treated sample, the treated and control membranes were gently removed from the UF cell at the end of the experiments (~4 days), cut to pieces of ~1 cm^2 and prepared for scanning electron microscopy (SEM) observation as detailed in Section 2. Fig. 6 presents representative SEM images of control and treated membrane surface after 106 h of sequential filtering through a 0.01-μm PC membrane. Image (A) shows, at this time, a layer of control cells interconnected with EPS, a typical image of biofilm cake [30]. The SEM picture is consistent with the cake filtration model presented in Fig. 5 for the control sample. Image (B) shows the treated membrane surface at the same magnification. The treated cells do not create a layer on the surface and interconnection between cells was not observed, however, deposition of NPs was observed. Energy-dispersive X-ray (EDX) spectroscopy, which enables determining the chemical composition of the deposition area, showed the presence of Ag. Other elements, such as Cl, P, Na, K, and other trace elements originating from the M9 medium were present on the control membrane as well as on the treated membrane. Image (B) demonstrates the absence of biofilm layer and the presence of two different particle deposition types (NPs and bacterial cells); resulting in a complex combined fouling mechanism. Indeed, the experimental treated data do not fit any of the individual classic models. Image (C) shows a higher magnification of the treated membrane surface and presents a lysed cell or traces of cells that were detached from the membrane during rinsing. Image (D) zooms in on one of the NPs deposition area.

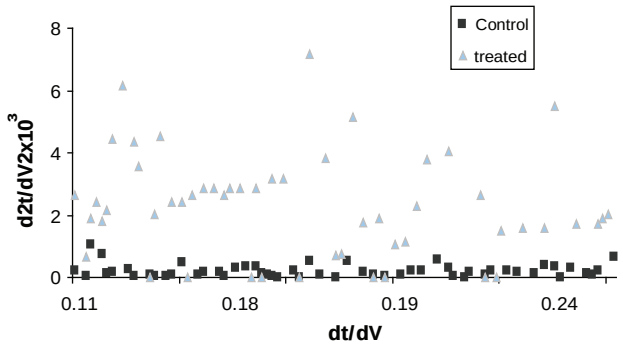

Fig. 5. The d^2t/dV^2 versus dt/dV for treated and control samples (mL/h).

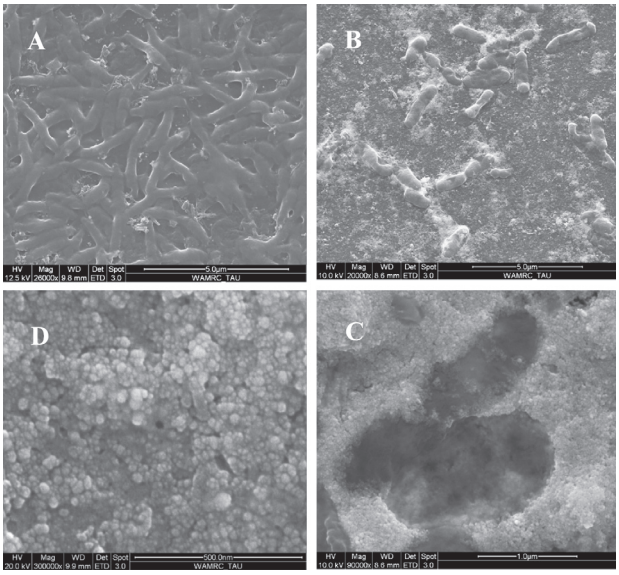

Fig. 6. SEM images of *P. aeruginosa* filtered through a PC membrane. Image (A) shows a layer of control cells; image (B) shows the treated sample at the same magnification. Images (C) and (D) are higher magnifications of Ag-NPs dense deposition area on the treated membrane. Scale bars are: (A,B) 5 μm, (C) 1 μm and (D) 500 nm.

4. Conclusions

To conclude:

- Exposure of bacterial cells to Ag-NPs results in less attached biomass.
- Exposure of bacterial cells to Ag-NPs results in lower biofouling buildup
- A combined blocking filtration model is required to determine the exact blocking laws that are involved in the process.

Acknowledgments

This research was supported in part by SWITCH (EU-funded research program). The authors acknowledge Prof. Gil Markovich and Tania Belenkova for their fruitful collaboration and insights on NPs, and thank Dr. Zahava Barkay for her assistance with the Scanning electron microscopy.

References

[1] H.C. Flemming, Biofouling in water systems – cases, causes and countermeasures. Appl. Microbiol. Biotechnol., 59 (2002) 629–640.
[2] P.L. Bishop, The role of biofilms in water reclamation and reuse. Water Sci. Technol., 55 (2007) 19–26.
[3] J.S. Baker and L.Y. Dudley, Biofouling in membrane systems – a review. Desalination, 118 (1998) 81–89.
[4] J. Kim and B. Van der Bruggen, The use of nanoparticles in polymeric and ceramic membrane structures: review of manufacturing procedures and performance improvement for water treatment. Environ. Pollut., 158 (2010) 2335–2349.
[5] S.Y. Lee, H.J. Kim, R. Patel, S.J. Kim, J.H. Kim and B.R. Min, Silver nanoparticles immobilized on thin film composite polyamide membrane: characterization, nanofiltration, antifouling properties. Polym. Adv. Technol., 18 (2007) 562–568.
[6] Y.H. Xiong and Y. Liu, Biological control of microbial attachment: a promising alternative for mitigating membrane biofouling. Appl. Microbiol. Biotechnol., 86 (2010) 825–837.
[7] A. Dror-Ehre, A. Adin, G. Markovich and H. Mamane, Control of biofilm formation in water using molecularly capped silver nanoparticles. Water Res., 44 (2010) 2601–2609.
[8] M.N. Moore, Do nanoparticles present ecotoxicological risks for the health of the aquatic environment? Environ. Int., 32 (2006) 967–976.
[9] J.S. Kim, E. Kuk, K.N. Yu, J.H. Kim, S.H. Park, H.J. Lee and S.H. Kim, Antimicrobial effects of silver nanoparticles. Nanomed-Nanotechnol., 3 (2007) 95–101.
[10] S. Shivastava, T. Bera, A. Roy, G. Singh, P. Ramachandrarao and D. Dash, Characterization of enhanced antibacterial effects of novel silver nanoparticles. Nanotechnology, 18(2007) 1–9.
[11] J.R. Morones, J.L. Elechiguerra, A. Camacho, K. Holt, J. Kouri, J.T. Ramirez and M.J. Yacaman, The bactericidal effect of silver nanoparticles. Nanotechnology, 16 (2005) 2346–2353.
[12] A. Kahru and H.C. Dubourguier, From ecotoxicology to nanoecotoxicology. Toxicology, 269 (2010) 105–119.
[13] K. Zodrow, L. Brunet, S. Mahendra, D. Li, A. Zhang, Q. Li and P.J.J. Alvarez, Polysulfone ultrafiltration membranes impregnated with silver nanoparticles show improved biofouling resistance and virus removal. Water Res., 43 (2009) 715–723.
[14] J.S. Taurozzi, H. Arul, V.Z. Bosak, A.F. Burban, T.C. Voice, M.L. Bruening and V.V. Tarabara, Effect of filler incorporation route on the properties of polysulfone-silver nanocomposite membranes of different porosities. J. Membr. Sci., 325 (2008) 58–68.
[15] H.L. Yang, J.C.T. Lin and C. Huang, Application of nanosilver surface modification to RO membrane and spacer for mitigating biofouling in seawater desalination. Water Res., 43 (2009) 3777–3786.
[16] J. Fabrega, J.C. Renshaw and J.R. Lead, Interaction of silver nanoparticles with *Pseudomonas putida* biofilms. Environ. Sci. Technol., 43 (2009) 9004–9009.
[17] W.M. Dunne, Bacterial adhesion: seen any good biofilm lately? Clin. Microbiol. Rev., 15 (2002) 155–166.
[18] A. Roosjen, H.J. Busscher, W. Norde and H.C. Van der Mei, Bacterial factors influencing adhesion of *Pseudomonas aeruginosa* strains to a poly (ethylene oxide) brush. Microbiology, 152 (2006) 2673–2682.
[19] E.T. Knudsen, G.N. Rolinson and R. Sutherland, Carbencillin: A new semisynthetic penicillin active against *Pseudomonas pyocyanea*. Brit. Med., 3 (1967) 75–78.
[20] M. Rosenberg, D. Gutnick and E. Rosenberg, Adherence of bacteria to hydrocarbons: a simple method for measuring cell-surface hydrophobicity. FEMS Microbiol. Lett., 9 (1980) 29–33.
[21] G.A. O'Tool and R. Kotler, Initiation of biofilm formation in Pseudomonas fluorescens WCS365 proceeds via multiple, convergent signalling pathways: a genetic analysis. Mol. Microbiol., 28 (1998) 449–461.
[22] C. Faille, C. Jullien, F. Fontaine, M.N. Bellon-Fontaine, C. Slomianny and T. Benezech, Adhesion of Bacillus spores and Escherichia coli cells to inert surfaces: role of surface hydrophobicity. Can. J. Microbiol., 48 (2002) 728–738.
[23] K.J. Hwang, C.Y. Liao and K.L. Tung, Analysis of particle fouling during microfiltration by use of blocking models. J. Membr. Sci., 287 (2007) 287–293.
[24] J. Hermia, Constant pressure blocking filtration laws—application to power-law non-Newtonian fluids. Chem. Eng. Res. Design., 60 (1982) 183–187.
[25] J.C. Crittenden, R.R. Trussell, D.W. Hand, K.J. Howe and G. Tchobanoglous, Water Treatment Principal and Design, 2nd ed, John Wiley & Sons, Inc.: Hoboken, New Jersey, 2005.
[26] W.D. Xu and S. Chellam, Initial stages of bacterial fouling during dead-end microfiltration. Environ. Sci. Technol., 39 (2005) 6470–6476.
[27] C.C. Ho and A.L. Zydney, A combined pore blockage and cake filtration model for protein fouling during microfiltration. J. Colloid. Interface. Sci., 232 (2000) 389–399.
[28] G. Bolton, D. LaCasse and R. Kuriyel, Combined models of membrane fouling: Development and application to microfiltration and ultrafiltration of biological fluids. J. Membr. Sci., 277 (2006) 75–84.
[29] B. Blankert, B.H.L. Betlem and B. Roffel, Dynamic optimization of a dead-end filtration trajectory: Blocking filtration laws. J. Membr. Sci., 285 (2006) 90–95.
[30] M. Whiteley, M.G. Bangera, R.E. Bumgarner, M.R. Parsek, G.M. Teitzel, S. Lory and E.P. Greenberg, Gene expression in Pseudomonas aeruginosa biofilms. Nature, 413 (2001) 860–864.